Journal of Ceramic Processing Research. Vol. 6, No. 3, pp. 218~222 (2005)

J O U R N A L O F
Ceramic Processing Research

Synthetic crossed-lamellar microstructures in oxide ceramics

Vikram S. Kaul and K.T. Faber*

Department of Materials Science and Engineering, Robert R. McCormick School of Engineering and Applied Sciences, Northwestern University, Evanston, IL, USA

A process has been developed to produce a crossed-lamellar-type microstructure in mullite combining tape casting, oriented lamination, and templated grain growth. Ceramic laminates were produced with aligned rod-like grains with the alignment direction varying from layer-to-layer with abrupt interfaces between layers. Other designed microstructures are also possible using this process.

Key words: mullite, tape casting, texture, templated grain growth, multilayer, x-ray diffraction.

Introduction

Many natural organisms produce ceramics such as bone, tooth and shell that can sustain high stresses, like those applied through impact or contact during wear [1]. Nature provides complex and organized microstructures in these ceramics to create tougher and more flaw-tolerant materials [2]. One specific example of an organism that creates a natural ceramic material is the giant pink Queen conch, *Strombus gigas*. The shell of *Strombus gigas* is composed of over 99.9% aragonite [2], arranged in a unique microstructure known as the crossed-lamellar microstructure (Fig. 1). This hierarchical microstructure consists of layers of ceramic lamellae over several length scales. The lamellae in each layer are aligned with the direction of alignment being perpendicular to lamellae in adjacent layers [2]. Previous work has shown that, as a result of this ordered and complex microstructure, this material exhibits enhanced toughness and flaw tolerance [3]. The energy-dissipating mechanisms employed in this system include multiple microcracking, crack bridging, crack blunting, and grain pull out [4].

In an effort to take advantage of and replicate existing ceramic microstructural designs, a process has been developed to create a modified version of the crossed-lamellar microstructure in mullite. Mullite was the chosen model ceramic material because of its anisotropic grain growth properties and desirable strength and creep resistance at high temperature [5]. Gönenli and Messing have previously shown that rod-like grains of mullite can be grown by seeding a mullite matrix with aluminum borate whisker templates [6].

*Corresponding author:
Tel : +1-847-491-2444
Fax: +1-847-491-7820
E-mail: k-faber@northwestern.edu

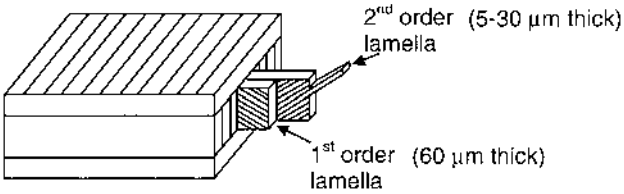

Fig. 1. Schematic of the crossed-lamellar microstructure seen in the shell of *Strombus gigas*, from Reference 4 (used with permission).

Although the process described here involves established ceramic processing techniques of tape casting, oriented lamination, and templated grain growth, this is the first time that the three methods have been used in concert to produce a crossed-lamellar microstructure. Tape casting serves as a method for making thin ceramic layers that can be stacked to form laminates. In addition, shear forces created during tape casting can be used to align anisotropic slurry particles in a single direction [7]. This, coupled with templated grain growth, provides a way to create a textured material with aligned grains in a controllable direction. The process is generic enough to fashion laminates with alignment that can vary arbitrarily between layers.

Experimental Procedure

Thin ceramic tapes used to produce the crossed-lamellar microstructure in mullite were cast from aqueous slurries. The ceramic components of the laminates were 82 vol.% $3Al_2O_3{\cdot}2SiO_2$, (KM-101, Kyoritsu Ceramics), 12 vol.% $9Al_2O_3{\cdot}B_2O_3$ whiskers (YS3a, Shikoku Chemicals), and 6 vol.% TiO_2 (Alfa Aesar). TiO_2 aids densification by serving as a liquid phase former during sintering and enhances anisotropic grain growth of mullite [8]. Densification to 92% of theoretical density is necessary before templated grain growth can occur [9]. The ceramic components made up 38

vol.% of the tape casting slurry. The non-ceramic components were 36 vol.% deionized water, 1 vol.% Darvan C dispersant (Vanderbilt Company), 5 vol.% polypropylene glycol plasticizer (Fluka), and 20 vol.% rhoplex b60-a polyacrylic emulsion binder (Rohm and Haas). The relative volume fractions of solvent, binder, and ceramic powder were carefully chosen to give optimal viscosity for casting and to maintain whisker alignment across the plane as well as through the thickness of the tape. The dispersant, binder, and plasticizer were chosen based on the work of Ushifusa and Cima [10].

Slurry components along with 10 mm alumina milling media were combined and ball milled for 24 hours, followed by de-airing prior to casting. The mullite tapes were manually cast with a modified doctor blade on a glass substrate covered with a polypropylene film. Flow of the slurry behind the blade was divided into 75 channels across the ~14 cm tape width by a flow divider. This was intended to increase the torque tending to align the aluminum borate whisker templates, which is proportional to n^2 where n is the number of channels [11]. The tape casting set up is shown in Figure 2a. Tapes were cast at 6 cm s^{-1} with a blade gap of 460 μm. Following casting, tapes were dried in air for approximately 1 hour. Dried tape thickness prior to lamination was ~300 μm.

Dried tapes were sectioned at +45° and –45° to the casting direction. Sections were then stacked with alternating ± 45° orientations as shown in Figure 2b. Each sample was composed of 20 layers. The tape stacks were then uniaxially pressed at room temperature with ~40 MPa pressure. Following the lamination and pressing, the organic components in the green laminates were burned out using heating rates and temperature holds determined from thermogravimetric analysis (TGA).

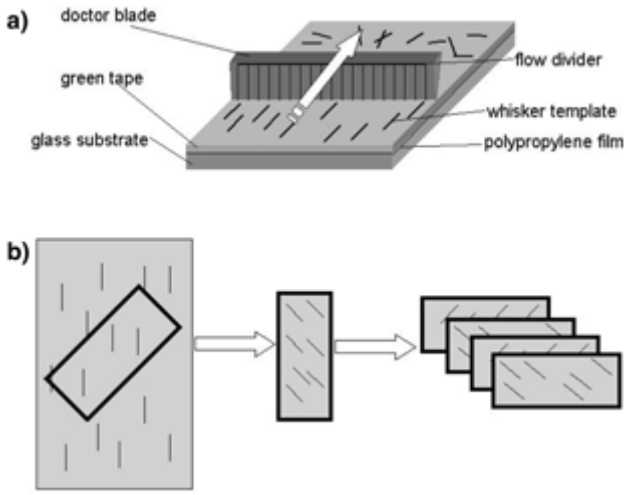

Fig. 2. Diagram of the a) tape casting setup showing aligned aluminum borate whisker templates in the mullite tape, and b) the sectioning of green tape with aligned whisker templates and ±45° stacking.

Samples were heated in a vented furnace to 220 °C at 3.5 K $minute^{-1}$, held at 220 °C for one hour, and further heated to 475 °C at 0.5 K $minute^{-1}$. Samples were then heated to 1000 °C at 3.5 K $minute^{-1}$, held at 1000 °C for 2 hours, and cooled to room temperature at 10 K $minute^{-1}$. The final heating step was necessary to ensure that the samples would be robust enough to handle following organic burnout. The laminates were then heated at 10 K $minute^{-1}$ to 1650 °C and sintered for 6 hours to allow for densification and anisotropic grain growth. Sintered samples were cooled to room temperature at 10 K $minute^{-1}$.

Scanning electron microscopy and optical microscopy (for greater contrast) were used to characterize morphological texture and to assess grain alignment in the samples in the casting plane and cross-section. Samples for microscopy were polished and thermally etched in air at 1550 °C for 12 minutes. X-ray diffraction was also used to characterize crystallographic texture and grain alignment. A Cu-Kα X-ray source with a 2 mm slit size was used for diffraction. Density of sintered materials was measured using Archimedes' principle [12]. Samples were also fractured in air at 1350 °C using a silicon carbide three-point bend fixture in a universal material tester at a rate of 0.4 mm/minute. Fracture surfaces were examined using the scanning electron microscope to observe crack propagation in relation to grain orientation.

Results and Discussion

Micrographs of mullite with aligned rod-like grains created by templated and untemplated mullite are shown in Figure 3. The templated mullite consists of long aligned rod-like grains of up to 100 μm in length while the untemplated mullite consists of fine equiaxed grains and elongated grains of up to 15 μm in length. The sintered mullite, templated and untemplated, was greater than 94% dense, based upon the theoretical density of mullite.* Due to the shear forces created during tape casting and the division of slurry flow, the long axes of the anisotropic aluminum borate whisker templates are aligned parallel to the casting direction [7].

Upon sintering, the aluminum borate whiskers encourage anisotropic grain growth within the mullite matrix through templated grain growth. The templates grow to consume the surrounding matrix and anisotropic rod-like mullite grains nucleate and grow to form a highly textured microstructure [9]. Due to the alignment of the aluminum borate whiskers during tape casting, the rod-like mullite grains in the sintered material are all aligned parallel to the tape casting direction. The whisker templates in the mullite matrix

*The percent density may be underestimated due to the presence of a lower density intergranular phase.

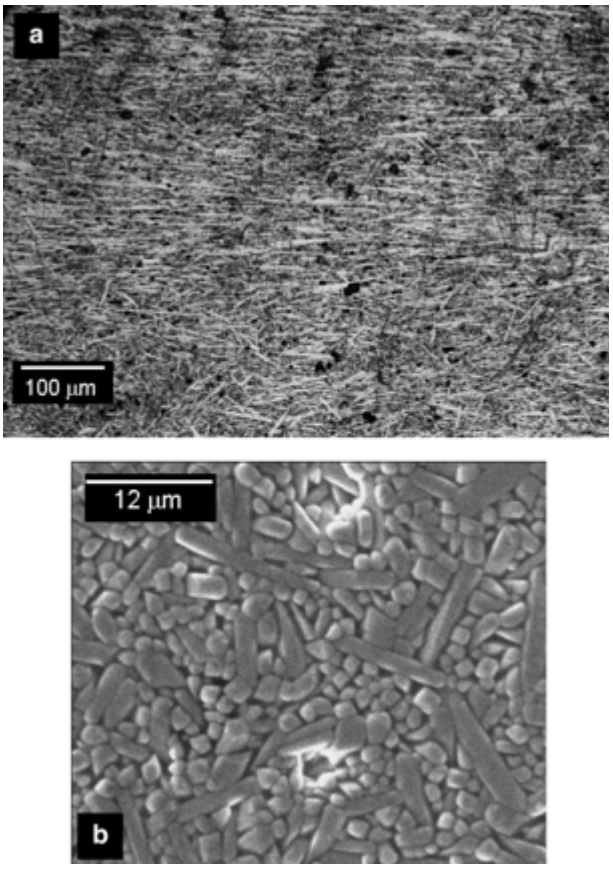

Fig. 3. Sintered microstructures in the tape casting plane of a) templated and b) untemplated mullite laminates by optical and scanning electron microscopy, respectively.

tend to decompose to Al_2O_3 and B_2O_3 [5]. Al_2O_3 is soluble in mullite, while B_2O_3 and TiO_2 tend to form glassy grain boundary phases observable by transmission electron microscopy [13, 14].

The process developed allows control of grain alignment between laminate layers so that the direction of alignment can change abruptly from one layer to the next. Sintering of green laminates with alternating $\pm 45^\circ$ template alignment produces a material with a microstructure similar to that of the middle layer of the crossed-lamellar microstructure seen in Fig. 1. In the sintered mullite, each layer is analogous to a first-order lamella and the individual rod-like mullite grains are analogous to second-order lamellae in the crossed-lamellar microstructure. Cross-sectioning this material at 45° shows layers in the laminate material with alternating alignment of the rod-like mullite grains at 0° and 90° (Fig. 4a). It is clear from Fig. 4a that alignment and texture is maintained through the thickness of each layer and that sharp interfaces exist between each layer, similar to the crossed-lamellar microstructure of *Strombus gigas*. Closer inspection of a layer interface shown in Figure 4b shows no delamination between layers.

In addition to morphological texture seen in optical and scanning electron micrographs, X-ray diffraction reveals clear crystallographic texture and serves as

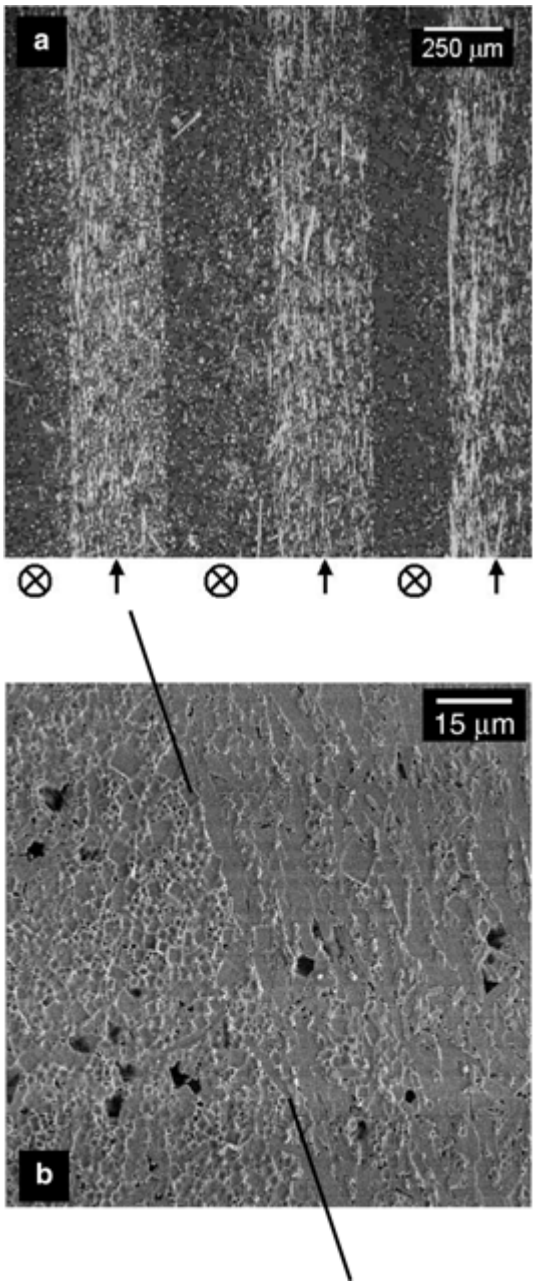

Fig. 4. a) Optical micrograph cross-section of a mullite laminate showing alternate grain alignment. Symbols represent the direction of grain alignment in each layer. b) SEM micrograph of the interface region showing the abrupt change of grain alignment.

another confirmation of grain alignment. Growth of the mullite grains is along the <001> direction as templated by the aluminum borate whiskers. The grain faces consist of {110} and {111} planes [15]. X-ray diffraction scans of the tape casting plane, and of the cross-section parallel to the direction of grain alignment are shown in Fig. 5 along with a scan of an untemplated sample. Fig. 5a shows a large peak corresponding to the (110) reflection and virtually no indication of the (001) and (002) reflections, showing the long axes of the mullite grains are in the tape casting plane. Figure 5b reveals

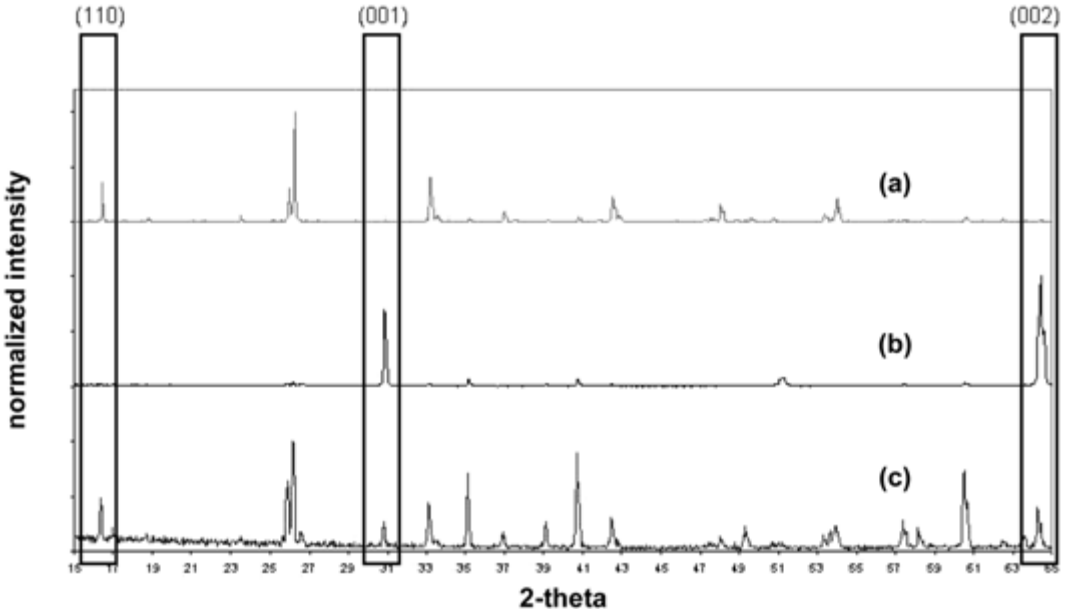

Fig. 5. X-ray diffraction scans of mullite laminates (a) of the tape casting plane, (b) the cross-section in the direction parallel to the long axis of the grains, and (c) the tape casting plane of untemplated mullite.

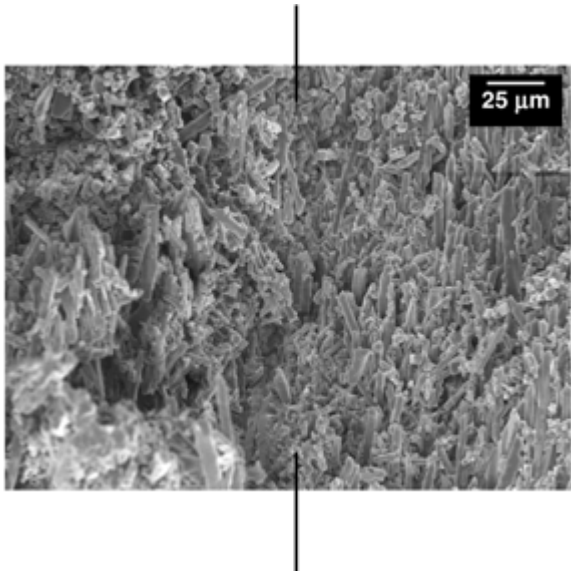

Fig. 6. Mullite laminate fracture surface showing crack path change at a layer interface (marked by the black lines). The direction of grain alignment shifts from –45° to +45° across the interface. The direction of crack propagation is from the bottom of the figure to the top.

the complement, as expected. These scans indicate that the preferred growth direction is <001> and that grains are well aligned in each layer.

Crack propagation in the mullite laminates can be observed by examining the fracture surface shown in Fig. 6. Samples were fractured at 1350 °C because mullite exhibits transgranular fracture at room temperature, but a mix of intergranular and transgranular fracture at high temperatures [16]. Figure 6 shows a change in crack path at a layer interface as the direction of grain alignment shifts from –45° to +45° across the interface, similar to fracture in *Strombus gigas* [3].

The process developed here can be readily applied to other ceramics where control of anisotropy is desirable. In addition to mullite, templated grain growth has been used to produce textured microstructures in many ceramics including alumina [9, 17], silicon carbide [18], silicon nitride [19], bismuth titanate [20], and barium hexaferrite [21]. The control of whisker alignment within layers through tape casting and between layers through oriented lamination allows for the creation of designed microstructures for heat conduction, electrical conduction, or in piezoelectric applications where anisotropy may be desired.

Conclusions

By combining tape casting, oriented lamination, and templated grain growth it is possible to produce a ceramic material that exhibits a simplified version of the crossed-lamellar microstructure. Mullite laminates produced through this process exhibit a microstructure of aligned rod-like grains with abrupt changes in the direction of grain alignment at layer interfaces. Both morphological and crystallographic texture was confirmed through microscopy and X-ray diffraction. High temperature fracture of this material results in tortuous crack paths as crack propagation changes directions as grain alignment shifts across the +45°/–45° interfaces. The process developed here can be further extended to ceramics for applications where control of anisotropy is important.

References

1. M. Sarikaya, Proc. Nat. Acad. Sci. 96[25] (1999) 14183-14185.
2. V.J. Laraia and A.H. Heuer, J. Am. Ceram. Soc. 72[11] (1989) 2177-2179.
3. T.J. Hill, "Quantitative Fracture Analysis of a Biological Ceramic Composite," Doctoral Dissertation. University of Florida (2001) p.55.
4. S. Kamat, X. Su, R. Ballarini, and A.H. Heuer, Let. to Nat. 405 (2000) 1036-1040.
5. I.A. Aksay, D.M. Dabbs, and M. Sarikaya, J. Am. Ceram. Soc. 74[10] (1991) 2343-2358.
6. I.E. Gönenli and G. L. Messing, J. Euro. Ceram. Soc. 21 (2001) 2495-2501.
7. G.L Messing, F. Lang, and S.-I. Hirano, "Ceramic Processing Science" (American Ceramic Society, 1998) p. 497.
8. S.H. Hong and G.L. Meesing, J. Am. Ceram. Soc. 82[4] (1999) 867-872.
9. E. Suvaci and G.L. Messing, J. Am. Ceram. Soc. 83[8] (2000) 2041-2048.
10. N. Ushifusa and M.J. Cima, J. Am. Ceram. Soc. 74[10] (1991) 2443-2447.
11. D.S. Park and C.W. Kim, J. Mat. Sci. 34 (1999) 5827-5832.
12. ASTM C373, "Standard Test Method for Water Absorption, Bulk Density, Apparent Porosity, Specific Gravity of Fired Whiteware Products" (ASTM International, 1999).
13. T. Huang, M. Rahaman, B. Eldred, and P. Ownby, J. Mater. Res. 16[11] (2001) 3223-3228.
14. H. Schneider, Ceram. Int. 13 (1987) 77-82.
15. T. Huang, M.N. Rahaman, T.-I. Mah, and T.A. Parthasarathay, J. Am. Ceram. Soc. 83[1] (2000) 204-210.
16. R. Torrecillas, G. Fantozzi, S. de Aza, and J. Moya, Acta Mater. 45[3] (1997) 897-906.
17. T. Carisey, I. Levin and D. Brandon, J. Euro. Ceram. Soc. 15[4] (1994) 283-289.
18. M. Sacks, G. Scheiffele, and G.J. Staab, J. Am. Ceram. Soc. 79[6] (1996) 1611-1616.
19. K. Hirao, M. Ohashi, M. Brito, and S.J. Kanzaki, J. Am. Ceram. Soc. 78[6] (1995) 1687-1690.
20. Y. Kan, P. Wang, Y. Li, Y. Cheng, and D. Yan, J. Euro. Ceram. Soc. 23[12] (2003) 2163-2169.
21. D.B. Hovis and K.T. Faber, Scripta Mat. 44 (2001) 2525-2529.